Process method to suppress the effect of phase errors in alternating phase shift masks

Navab Singh[a)]

*Institute of Microelectronics, 11 Science Park Road, Singapore Science Park II, Singapore 117685
and Department of Electrical and Computer Engineering, National University of Singapore,
4 Engineering Drive 3, Singapore 117576*

Moitreyee M. Roy and Sohan S. Mehta

Institute of Microelectronics, 11 Science Park Road, Singapore Science Park II, Singapore 117685

A. O. Adeyeye

*Department of Electrical and Computer Engineering, National University of Singapore, 4 Engineering
Drive 3, Singapore 117576*

We have developed a process method to suppress the effect of phase errors in alternating phase shift masks. Our method uses double exposure at reversed focus offsets to nullify the intensity imbalance caused by the phase errors. We have evaluated our technique using 120 nm half-pitch line space patterns and found it very successful with remarkable improvement in usable depth of focus without loosing exposure latitude. We also observed that our technique could bring immunity against the lens aberrations such as defocus and astigmatism. © 2005 American Vacuum Society.
[DOI: 10.1116/1.1885012]

I. INTRODUCTION

The resolution enhancement in optical lithography using alternating phase shift mask (alt-PSM) is well-known in the semiconductor industry. It results in the best resolution enhancement but at the cost of tremendous complications in data preparation and mask fabrication. Other than phase conflicts, the issues in using alt-PSM are transmission and phase errors. The transmission error is mainly a result of improper biasing between zero and π phase apertures and, therefore, can be corrected easily. The phase error which is caused by the deviation in quartz etch-depth is difficult to control precisely. These errors cause intensity imbalance between zero and π phase apertures which leads to critical dimension (CD) nonuniformity or misplacement of patterns on the wafer.[1,2] The side wall scattering in the etched trenches also play a role in the intensity imbalance.[3] Rigorous electromagnetic theories have already been used to model the scattering in case of phase shift masks.[4,5] Dual trench method can be used as a partial solution, however, the image log slope (a metric for aerial image qualification) decreases.[6] The intensity imbalance issue is now overcome using a sidewall chrome alternating aperture (SCAA) mask,[7,8] which has a good performance without shifter depth and space width adjustments. However, the SCAA masks are very expensive due to complicated mask fabrication steps. Shoji *et al.*[9] have suggested a very simple reversed phase double exposure method which is easy to implement but reduces the throughput to one fourth of the single exposure method. The throughput reduction is due to splitting of the exposure field into two parts and exposing them one by one on top of each other.

In this article, we present a process method to overcome phase error issues in phase shift masks. Our method uses double exposure at reversed focus offsets to nullify the intensity imbalance caused by the phase error. Using PROLITH (lithography simulator from KLA tencor), we have simulated our concept for $-10°$ phase error on 120 nm half-pitch alternating phase line space patterns and found it to work. We have experimentally validated it using 120 nm half-pitch line space patterns on alt-PSM fabricated at HOYA Corporation Japan and found remarkable improvement in usable depth of focus (UDOF) without loosing exposure latitude. We have also compared our method with the reversed phase double exposure technique presented by Shoji *et al.*[9] We observed that our technique could bring immunity against the lens aberrations such as defocus and astigmatism.

II. THEORETICAL ASPECTS

In imaging using alt-PSM, the diffraction orders are symmetrically placed from the lens center at a distance of half of the corresponding order with the binary mask having the same physical pitch. The reduction in angular separation of the diffraction orders increases the resolution. Furthermore, in ideal alt-PSM the zeroth diffraction order is missing which results in improved contrast. Also, the missing zeroth order creates the natural immunity to defocus when the image is formed using only first diffraction orders, which is typically the case in optical lithography at the resolution limit. The transmission or phase errors in the alt-PSM mask introduce zeroth diffraction order which then also participates in the image formation. The zeroth diffraction order due to transmission error acts like a focus noninteractive electric field flare. The zeroth order due to phase error acts like a focus interactive electric field flare. However, at zero defocus, it is orthogonal to the first orders and, therefore, behaves like an

[a)]Electronic mail: navab@ime.a-star.edu.sg
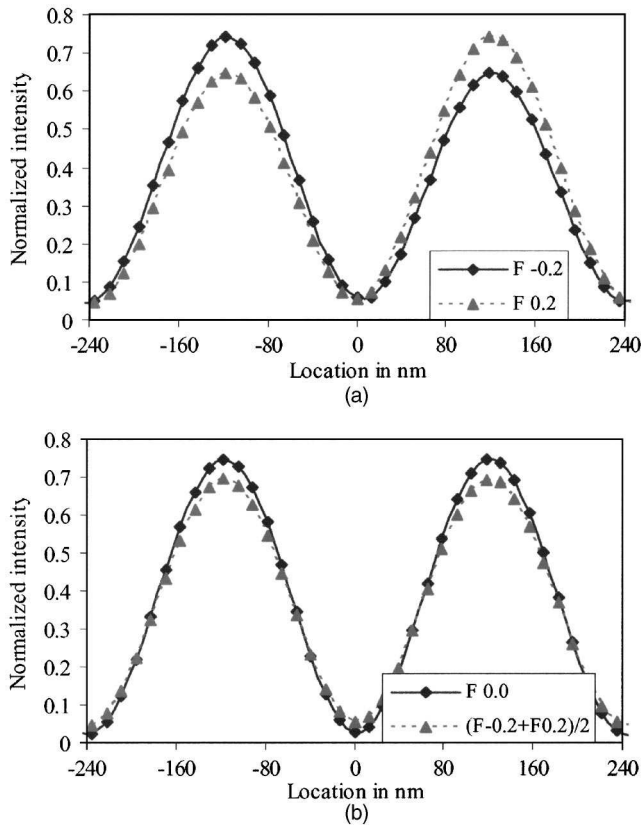
FIG. 1. PROLITH simulated normalized aerial image plots with a phase error of $-10°$—alternate apertures with 170° phase transmission instead of 180°. (a) Exposed at -0.2 and 0.2 μm focus offsets independently and (b) Zero defocus and opposite foci double exposure at -0.2 and 0.2 μm, respectively.

intensity flare. Defocus makes the phase-error-generated zeroth order to interfere with higher orders, which favors the zero-phase field on one side of best focus while the π phase field is on the other side. This phenomenon, therefore, results in reciprocal image intensity imbalance between zero phase and π phase apertures across the focus. Because of reciprocity across focus we found that the phase imbalance could be eliminated by a double exposure technique that uses reversed focus offsets on two different exposures. The intensity imbalance created at one focus is compensated when a second exposure is performed with the reversed focus.

In our article, we have only dealt with phase error through double exposure. Chris Mack[10] has shown that the out of focus intensity could be given by the relationship in Eq. (1):

$$I_{\text{out-of-focus}}(x, \nabla) \approx \left(1 - \frac{\Delta\varphi^2}{4}\right)I_{\text{ideal}}(x) + \Delta\varphi^2\left(\frac{w_s}{p}\right)^2$$
$$+ 2\Delta\varphi\left(\frac{w_s}{p}\right)E_{\text{ideal}}(x)\sin(\nabla), \tag{1}$$

where w_s, p, $\Delta\varphi$ are the space width, pitch, and phase errors, respectively. The symbol ∇ is the defocus angle which is proportional to the defocus distance for small values of defocus. The $E_{\text{ideal}}(x)$ and $I_{\text{ideal}}(x)$ are the electric field and intensity in case of an ideal mask without any phase and transmission error and are given by the following relations [Eqs. (2) and (3)].

$$E_{\text{ideal}}(x) = \frac{4}{\pi} \sin \frac{\pi w_s}{p} \cos kx, \tag{2}$$

$$I_{\text{ideal}}(x) = E_{\text{ideal}}(x)E_{\text{ideal}}^*(x), \tag{3}$$

where E^* is the complex conjugate of E.

From Eq. (1) it is obvious that $I_{\text{out-of-focus}}$ is a function of the defocus angle ∇. Moreover, the change of sign of the defocus angle from plus to minus and vice versa, changes the sign of last the term in Eq. (1), which is the only focus dependent term. Therefore, one can write the equation for average intensity in dual exposure as

$$I_{\text{average}} = \frac{1}{2}\{I_{\text{out-of-focus}}(x, \nabla) + I_{\text{out-of-focus}}(x, -\nabla)\}$$
$$\approx \left(1 - \frac{\Delta\varphi^2}{4}\right)I_{\text{ideal}}(x) + \Delta\varphi^2\left(\frac{w_s}{p}\right)^2. \tag{4}$$

Equation (4) is independent of the defocus term which shows that defocus related intensity imbalance caused by the presence of phase error can be eliminated by the dual exposure process. The two exposures have to be with reversed focus values.

III. SIMULATIONS AND EXPERIMENTAL

We did simulations using PROLITH on 120 nm line space patterns in alt-PSM with $-10°$ phase error—alternate apertures with 170° phase transmission instead of 180°. The aerial image intensity was simulated at the focus offsets of -0.2, 0.0, and 0.2 μm using single and double exposures. We validated our concept using a single trench alt-PSM reticle with 120 nm line space patterns at a duty ratio of 1:1. A global biasing of 20 nm was included besides undercut for the π phase features at the time of reticle fabrication in an effort to offset the transmission imbalance. The average and range phase values on the reticle measured using MPM-248 were 181.81° and 1.21°, respectively. We conducted all patterning experiments on 8 inch silicon wafers using Nikon KrF scanner S203 in line with a TEL Act-8 wafer track. The highest numerical aperture of 0.68 in our tool was used with the lowest available partial coherence of 0.31. The wafers were first coated with 4100 Å deep ultraviolet (DUV) resist on top of 600 Å thick layer of bottom antireflection coating (BARC). The focus exposure matrices (FEMs) were exposed on the wafers under three different categories, namely: Single exposure, reversed phase double exposure, and reversed focus double exposure. In single exposure the FEM was done using the standard FEM method by changing the dose and focus in rows and columns, respectively, or vice versa. The reversed phase double exposure was carried out by exposing the FEM twice but with 240 nm x shift in the second exposure with respect to the first. The shift value was equal to the pitch of the pattern in the x direction on the wafer so that each trench could be exposed twice, first
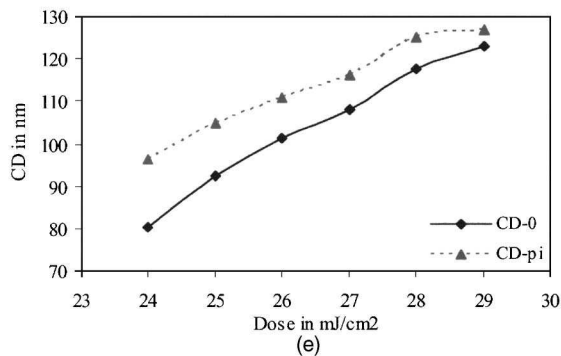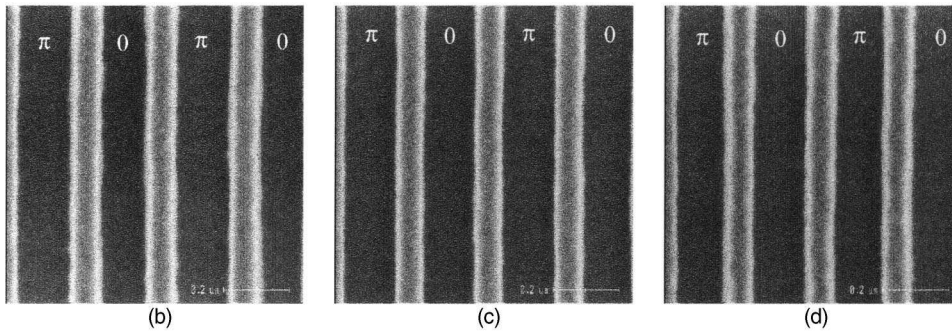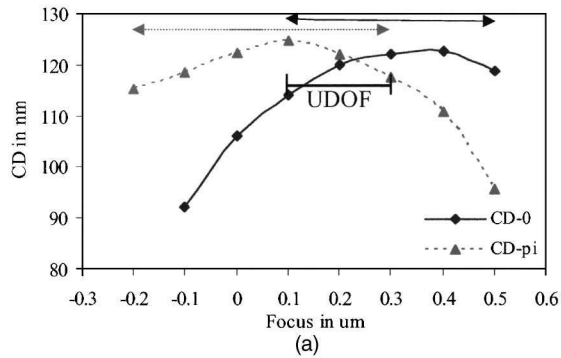
FIG. 2. Single exposure plots and images. The pitch value is 240 nm at a duty ratio 1:1. (a) Focus plots corresponding to 0 and π phases apertures at a dose of 29 mJ/cm^2. The solid and dashed arrowed horizontal lines represent the DOF corresponding to zero and π phase trenches, respectively. The thick horizontal line is showing the UDOF, (b) the top view SEM image at negative defocus (0.0 μm), (c) the top view SEM image at best focus (0.2 μm), (d) the top view SEM image at positive defocus (0.4 μm), and (e) the exposure dose plots corresponding to 0 and π phases apertures at best focus (0.2 μm).

through zero field and the second time through π field or vice versa. The reversed focus double exposure was carried out by exposing the FEM twice but with opposite focus offsets. The focus value reversal was done by changing the sign of the focus step in the second exposure. In both the double exposure methods the resist coating, soft bake, post exposure bake, and development were done only once and all these steps were kept the same for a direct comparison with the single exposure methods. Also the wafer was not unloaded from the stage after the first exposure to ensure the minimum misalignment between the two exposures. The total dose of double exposure was kept the same as a of a single exposure. In our experiment the focus step of ± 0.1 μm was given with a total exposure step of 1 mJ/cm^2. We performed the CD measurements using HITACHI CDSEM S9200. For each focus and dose values we measured the trenches corresponding to 0 and π phase apertures of the mask to study the effect of the interaction of focus and phase error on the patterning of trenches.

IV. RESULTS AND DISCUSSIONS

A. Validation of reversed foci double exposure concept through simulations

Shown in Fig. 1 are the PROLITH simulated aerial image plots with a phase error of $-10°$—alternate apertures with $170°$ phase transmission instead of $180°$ (under etch of π phase space). It is clear from Fig. 1(a) that with $-10°$ phase error a defocus of ± 0.2 μm has created ~ 0.1 intensity imbalance between zero and π phase apertures. At negative defocus the peak intensity through the π phase space is more than the peak intensity through zero phase space. The converse is true at positive defocus (not shown). It is the outcome of constructive and destructive interference depending upon the phase. The effect of negative and positive defocus will interchange if the phase error is positive—over each of the π phase space. The zero defocus and opposite foci (-0.2 and 0.2 μm) double exposure simulation results are shown in Fig. 1(b). As theoretically explained in Sec. II, both the
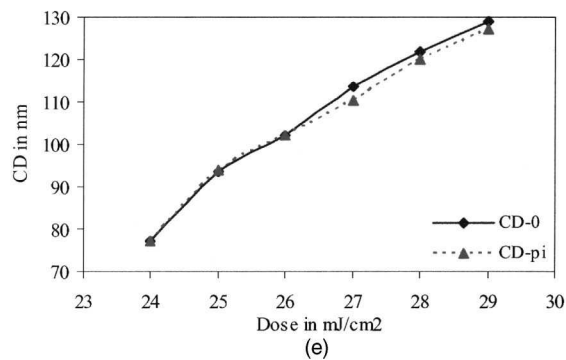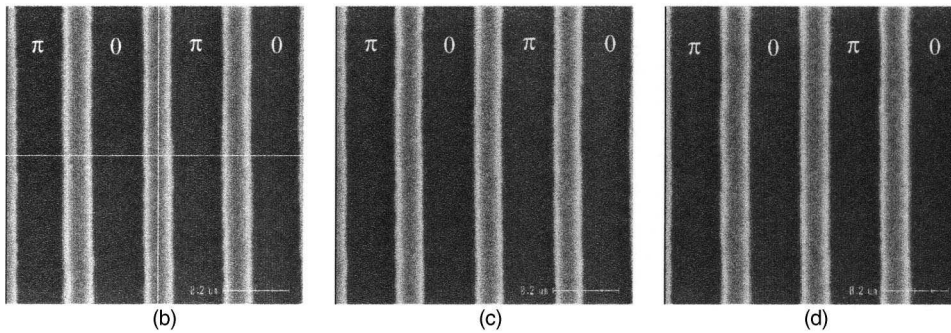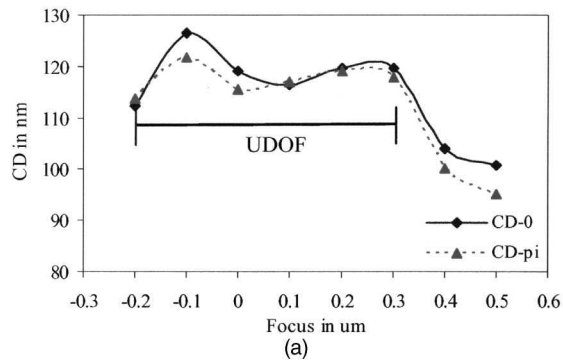
FIG. 3. Reversed phase double exposure plots and images. The pitch value is 240 nm at a duty ratio 1:1. (a) Focus plots corresponding to 0 and π phases apertures at total dose of 28 mJ/cm^2. DOF of zero and π phase aperture is common and displayed as UDOF by the thick horizontal line, (b) the top view SEM image at negative defocus (-0.1 μm), (c) the top view SEM image at best focus (0.1 μm), (d) the top view SEM image at positive defocus (0.3 μm), and (e) the exposure dose plots corresponding to 0 and π phases apertures at best focus (0.1 μm).

curves are free from intensity imbalance despite the $-10°$ phase error in the mask. However, a little reduction in contrast is noticed in the case of the opposite foci double exposure method. A direct comparison of intensity plots in Figs. 1(a) and 1(b) demonstrate that the phase error generated intensity imbalance could be eliminated using reversed foci double exposure. Next, we now present the experimental verification of this fact.

B. Effect of phase error in single exposure method

Shown in Fig. 2 are the focus plots, top view SEM images and exposure plots of 120 nm half-pitch trenches using alt-PSM with a single exposure. The focus plots shown in Fig. 2(a) are quite interesting in the sense that at negative defocus (<0.2 μm) the π phase trench is wider than zero phase trench while the converse is true for positive defocus. This is qualitatively matching with negative ($-10°$) phase error simulation and, therefore, is an indication of the under etch of π phase trenches in the mask making. Because of the phase error the usable depth of focus (UDOF) has reduced almost by 0.2 μm—change in DOF of zero or π phase to

zero and π phase. The top view SEM images corresponding to negative defocus (0.0 μm), best focus (0.2 μm) and positive defocus (0.4 μm) are shown in Figs. 2(b)–2(d), respectively. The SEM images also reflected the CD imbalance with focus. Based on these results, one may conclude that if the wafer is exposed at a focus offset of 0.2 μm, the CD uniformity on the wafer would be quite good if there is no drift in focus and tilt, provided the wafer is flat. However, if the wafer is not flat, or there are some drifts in focus or tilt, the two adjacent trenches (zero and π phase) could easily have CD differences in the range of 10–20 nm. Figure 2(e) shows the exposure plots at best focus (0.2 μm) on 120 nm half-pitch trenches using alt-PSM with single exposure. It also illustrates a delta between the CDs of 0 and π phase trenches. However, the delta has decreased with increasing dose. The reduction in CD delta with overdose is attributed to the lowering of threshold towards the bottom of the aerial image where the effect of phase error is least. This experiment thus demonstrates the presence of negative phase error on the mask.

(a)

(b)

(c)

(d)
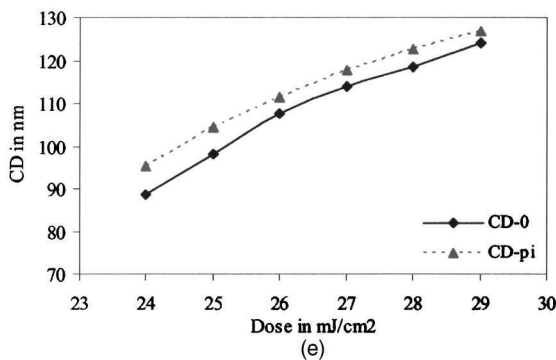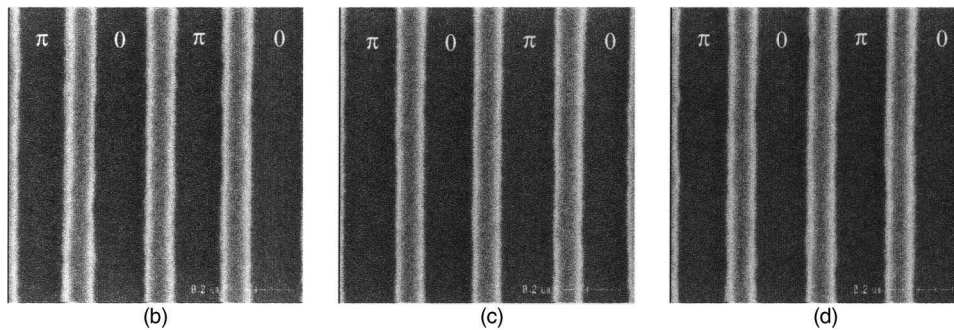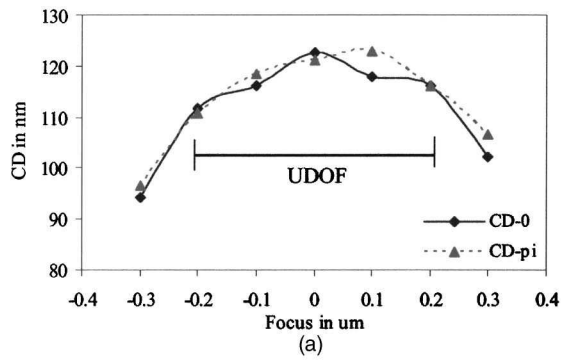
FIG. 4. Reversed focus double exposure plots and images. The pitch value is 240 nm at a duty ratio 1:1. (a) Focus plots corresponding to 0 and π phases apertures at total dose of 28 mJ/cm^2. DOF of zero and π phase trenches is common and displayed as UDOF by the thick horizontal line, (b) the top view SEM image at negative defocus (0.2 μm), (c) the top view SEM image at best focus (0.0 μm), (d) the top view SEM image at positive defocus (0.2 μm), and (e) the exposure dose plots corresponding to 0 and π phases apertures at best focus (0.0 μm).

(e)

C. Suppression of the phase error effects using reversed phase double exposure method

Shown in Fig. 3 are the focus plots, SEM images and exposure plots of 120 nm half-pitch trenches using alt-PSM with reversed phase double exposure method. In contrast to the single exposure the reversed phase double exposure method is almost immune to the phase errors. The focus plots shown in Fig. 3(a) demonstrate that the 0 and π phase trenches have almost comparable CDs across the focus. The UDOF has increased to 0.5 μm with a best focus at 0.1 μm. The top view SEM images corresponding to negative defocus (-0.1 μm), best focus 0.1 μm, and positive defocus (0.3 μm) are shown in Figs. 3(b)–3(d), respectively. The SEM images show the elimination of CD imbalance as the adjacent trenches are equal in all the three images. However, as shown in Fig. 3(e), the exposure latitude (inverse slope of the CD versus exposure dose plots) has slightly reduced in comparison to the single exposure case. We have thus shown that the effect of phase error on the mask could be well suppressed by reversed phase double exposure with very little loss in exposure latitude.

D. Suppression of the phase error effects using reversed foci double exposure method

Shown in Fig. 4 are the focus plots, SEM images and exposure plots of 120 nm half-pitch trenches using alt-PSM with reversed focus double exposure method. A focus-exposure matrix was constructed with same exposure dose on both exposures but with the focus reversed. This led to the negative defocus overlapped with positive defocus of the same amount. As can be seen from focus plots in Fig. 4(a), similar to the reversed phase double exposure technique, the reversed focus double exposure method is also immune to the phase errors. The zero and π phase trenches have fully overlapped focus plots. The UDOF is 0.4 μm, which is 0.2 μm more than the single exposure case. The top view SEM images corresponding to negative defocus (-0.2 μm), best focus (0.0 μm) and positive defocus (-0.2 μm) are shown in Figs. 4(b)–4(d), respectively. The SEM images also show the elimination of CD imbalance as the adjacent trenches are equal in all the three images. The exposure plots shown in Fig. 4(e), demonstrate that the exposure latitude is comparable to the single exposure case. However, there is a

FIG. 5. The top view SEM images of L-bars showing suppression of astigmatism using reversed foci double exposure. (a) Single exposure at negative defocus (0.0 μm), (b) single exposure at positive defocus (0.3 μm), (c) reversed foci double exposure at focus$=-0.2$ μm, and (d) reversed foci double exposure at focus$=0.2$ μm.

posure technique could suppress the astigmatism effect on the patterning. The Z5 and Z6 terms of the Zernike polynomials are optical path difference (OPD) surfaces with the shape of humps positively and negatively in two orthogonal directions. In line space patterns, pure Z6 introduces a focus difference between the lines in horizontal and vertical directions while Z5 introduces the difference in $+45°$ and $-45°$ orientations. We have seen the astigmatism effect in our scanner lens as shown through Figs. 5(a) and 5(b) by comparing the SEM images at negative and positive focus offsets of an L bar pattern. At negative focus the vertical line space patterning near the 90° bending is bad (scum between the lines) while the horizontal pattering is bad at positive focus offset. Shown in Figs. 5(c) and 5(d) are the top view SEM images of the same L bar pattern exposed using reversed foci technique. The suppression of the astigmatism effect is obvious as the L bar patterning is the same on both sides of best focus.

In term of CD nonuniformity suppression, our technique could produce the results comparable to previously published reversed phase method. Moreover our technique is superior to reversed phase in term of throughput—the reversed focus method can use full reticle field while the reversed phase can use only half as duplication of pattern is required, and astigmatism suppression. Once the phase imbalance is compensated the remaining imbalance from transmission, the focus noninteractive part, could be easily corrected by additional biasing to one of the phases.

V. CONCLUSIONS

We observed that the CD nonuniformity caused by phase error induced intensity imbalance in an alternating phase shift mask could be corrected using the reversed foci double exposure technique. The DOF of the opposite phases overlap on each other minimizing the CD difference that showed up as a result of phase imbalance. It also resulted in a considerable increase in usable depth of focus. The reversed foci double exposure method has proved quite beneficial for compensating certain lens aberrations that are focus dependent, such as astigmatism. In this technique the effect of double exposure on exposure latitude was also found negligible. Lastly it can be said that this technique gives numerous advantages over existing methods and can be implemented quite easily in a manufacturing environment.

uniform CD delta between zero and π phase trenches which would require zero- π bias adjustment on the mask. Thus, through this experiment we confirm that the effect of phase error on the mask could be well suppressed by reversed focus double exposure with no loss in exposure latitude.

We observed that, in addition to the elimination of phase error related image imbalance, our reversed foci double ex-

[1]J. S. Peterson *et al.*, BACUS News: Photomask, **14**, Issue 8 (Aug 1998).
[2]R. Kostelak, C. Pierrat, J. Garofalo, and S. Vaidya, J. Vac. Sci. Technol. B **10**, 3055 (1992).
[3]C. Pierrat, A. Wong, and S. Vaidya, in Tech. Digest-International Electron Devices Meeting (Dec. 1992), pp. 53–56.
[4]A. Wong and A. Neureuther, IEEE Trans. Electron Devices **41**, 895

(1994).

[5]K. Lucas, A. Strojwas, K. Low, and C. Yuan, Proc. SPIE **1927**, 438 (1993).

[6]T. Terasawa, N. Hasegawa, A. Imai, and S. Okazaki, Jpn. J. Appl. Phys., Part 1 **34**, 6578 (1995).

[7]M. D. Levenson, J. S. Petersen, D. J. Gerold, and C. A. Mack, Proc. SPIE **4186**, 395 (2001).

[8]M. D. Levenson *et al.*, Proc. SPIE **4346**, 817 (2001).

[9]Shoji Hotta *et al.*, Proc. SPIE **5377**, 545 (2004).

[10]Chris A. Mack, Microlithogr. World **12**, 16 (2003).